Atmósfera 39, 629-654 (2025)
https://doi.org/10.20937/ATM.53464

Modeling climate change impacts on the Nazas River basin: Future aridity and land use change

Gabriel de Jesús PEÑA-URIBE[1], Oscar VALDIVIA-MARTÍNEZ[2], Gabriel Fernando CARDOZA-MARTÍNEZ[1], Fernando ALONZO-ROJO[1] and Armando LÓPEZ-SANTOS[3]*

[1] *Facultad de Ciencias Biológicas, Universidad Juárez del Estado de Durango, Av. Universidad s/n, Núcleo Universitario, Col. Filadelfia, 35019 Gómez Palacio, Durango, México.*
[2] *Universidad Rosario Castellanos. Av. 506 0, Col. San Juan de Aragón II Sección, 07969 Ciudad de México, México.*
[3] *Unidad Regional Universitaria de Zonas Áridas, Universidad Autónoma Chapingo, km 40 carretera Gómez Palacio-Ciudad Juárez, Bermejillo, 35230 Mapimí, Durango, México.*
*Corresponding author; email: alopez@chapingo.uruza.edu.mx

Received: December 10, 2024; Accepted: August 26, 2025

RESUMEN

Este estudio evaluó los posibles cambios de aridez en la cuenca del río Nazas (CRN), utilizando el índice de aridez de De Martonne, datos históricos (1970-2000) y proyecciones de cuatro modelos climáticos dentro de dos trayectorias socioeconómicas compartidas (SSP1-2.6 W m^{-2} y SSP5-8.5 W m^{-2}) y dos horizontes temporales (2021-2040 y 2041-2060). Además, se analizaron las perturbaciones antrópicas comparando los cambios en el uso del suelo y la cobertura vegetal (USCV) entre 2003 y 2018. Los resultados indican que el 64 % de la CRN es árida. Los modelos climáticos proyectan una aridez creciente, pero solo el modelo CNRM-CM6-1 muestra cambios estadísticamente significativos con el SSP1 (2041-2060) y el SSP5 (para ambos periodos). El escenario CNRM-CM6-1 SSP5 (2041-2060) proyecta un aumento de la aridez de hasta el 81 %, lo que sugiere que el 29 % de la CRN, principalmente en la parte superior, podría estar amenazado por una mayor aridez. La categoría de aridez más severa proyectada fue semiárida, sin expectativas de que alcance condiciones hiperáridas a mediano plazo. No hubo diferencias estadísticamente significativas del USVC entre 2003 y 2018; sin embargo, los asentamientos humanos se expandieron con una tasa de crecimiento anual del 6.6 %, comparable con la de algunas ciudades importantes de Asia. Aunque cubren una pequeña área de la cuenca, los asentamientos humanos desempeñan un papel importante en el forzamiento radiativo. El aumento de tierras productivas, principalmente de cultivo, podría afectar la retención de CO_2 y los procesos hidrodinámicos del suelo, incrementando la vulnerabilidad a la erosión y la probabilidad de desertificación.

ABSTRACT

This study assessed potential aridity shifts in the Nazas River basin (NRB) using the De Martonne Aridity Index, historical data (1970-2000), and projections from four climate models under two shared socioeconomic pathways (SSP1-2.6 W m^{-2} and SSP5-8.5 W m^{-2}) and two time horizons (2021-2040 and 2041-2060). Additionally, anthropogenic disturbances were analyzed by comparing changes in land use and vegetation cover (LUVC) between 2003 and 2018. Results show that 64% of the NRB is currently arid. Climate models project increasing aridity, but only the CNRM-CM6-1 model shows statistically significant changes under SSP1 (2041-2060) and SSP5 (for both periods). The CNRM-CM6-1 model under the SSP5 (2041-2060) scenario projects an increase in aridity of up to 81% (54% for Mediterranean semiarid climate and 27% for semiarid climate), suggesting that 29% of the NRB, mainly in the upper part, could be threatened by increased aridity. The most severe aridity category projected was semiarid, with no expectation of reaching hyper-arid conditions in the medium term. LUVC changes between 2003 and 2018 showed no statistically significant differences. However, human settlements expanded with an annual growth rate of 6.6%, comparable to that of

some major cities in Asia. Although covering a small area of the basin, human settlements play a significant role in radiative forcing. The increase in productive lands, mainly croplands, could impact CO_2 retention and soil hydrodynamic processes, increasing susceptibility to erosion and the likelihood of desertification.

Keywords: climate modelling, land use change, arid basin, Mexico, Radiative forcings.

1. Introduction

Global warming of the atmosphere and surface of the oceans and continents, due to human influence, is a fact (IPCC, 2021). Furthermore, climate change (CC) hazards are primarily driven by anthropogenic factors, including greenhouse gas (GHG) emissions, deforestation, overgrazing, and high-pressure water use, among others (Lawrence et al., 2023). This has caused changes in salt concentrations on the surface of the oceans; a 40% decrease in continental and maritime glaciers in the Arctic from 1979 to 2019 (UNEP, 2019); an increase in the average sea level (approximately 0.2 m) between 1901-2018, with a mean rate of 1.3 mm year^{-1}, and a shift in climatic zones towards the poles, among others (IPCC, 2021). Furthermore, climate change influences extreme hydrometeorological events worldwide. For this reason, it is widely regarded as the most significant challenge to the permanence of natural and human systems globally (UNTFHS, 2017; IPCC, 2022).

Due to CC, aridity is one of the biggest environmental problems around the world (Huang et al., 2015a). Climatic zones, such as drylands, are likely among the most disturbed at local, regional, and global scales. These impacts affect environmental patterns and human activities (Li et al., 2021; Jafarpour et al., 2023; Lugoi et al., 2023). Some studies mention that, in no more than three decades, drylands have expanded globally by about 9%, and by the end of this century, the expansion could be even greater (Feng and Fu, 2013; Huang et al. 2015a, 2017; Cherlet et al., 2018; IPCC, 2021; Ullah et al., 2022; Zhang et al., 2024) to cover 50% of the earth's surface (Huang et al., 2015b).

The Nazas River basin (NRB) is one of the largest and most complex hydrological basins in north-central Mexico (Descroix et al., 1993; Salas-Quintanal, 2011). It is an endorheic basin whose waters originate in the Sierra Madre Occidental, northwest of the state of Durango, from two main tributary rivers: Sextín and Ramos. Both flow into the Lázaro Cárdenas dam, continuing as the Nazas River until the lagoons of Mayrán and Viesca in the state of Coahuila, which is why this region is known as the Comarca Lagunera (CL). Currently, the CL lagoons have not received water since the mid-20th century due to the construction of hydraulic infrastructure for irrigation and flow control, which was intended to protect the population of the main cities along the Nazas River (SEMARNAT, 2008).

The first section of the lower NRB received a conservation decree in 2004 under the name "Cañón de Fernández State Park, which was declared a Ramsar site in 2008 and subsequently designated as a Natural Resources Protection Area ("Ríos y Montañas de la Comarca Lagunera"; SEMARNAT, 2024). Furthermore, the NRB contributes about 89% of the surface water of Hydrological Region 36 (Descroix, 1993). Therefore, the Nazas River has exerted a significant influence on the livelihoods and economic activities (agriculture, agro-industrial, cattle raising, metallurgical mining, and even business tourism) of the CL (Salas-Quintanal, 2011).

In this context, some studies (Neri and Magaña, 2016; Murray-Tortarolo et al., 2018; Ortega-Gaucín et al., 2018a, b; Haro et al., 2021; Monterroso-Rivas and Gómez-Díaz, 2021) have reported part of the climate change hazards due to the predisposition of northern Mexico to droughts and water scarcity. Most studies on the NRB have focused on changes in precipitation averages (Cerano-Paredes et al., 2011, 2012; González-Barrios et al., 2011; Ezquivel-Arriaga et al., 2017). However, more attention is being paid to temperatures as a factor of aridity, rather than just the change in rainfall regime (Overpeck and Udall, 2020).

Other studies of the CL (López-Santos et al., 2013; López-Santos and Martínez-Santiago, 2015; Galloza et al., 2017) have conducted modeling to investigate potential changes in aridity due to climate change in certain municipalities of Durango state, including Lerdo, Gómez Palacio, and Mapimí. Additionally, Martínez-Sifuentes et al. (2023) have examined

the potential effects on evapotranspiration within a sub-basin located in the upper region of the NRB. Other studies in this area (Bueno-Hurtado et al., 2017; Graciano-Ávila et al., 2019; Morales-Inocente et al., 2020) have focused on changes in land use and land cover and their GHG dynamics (capture/emission) in forest lands, but do not specifically address the impacts of aridity on NRB.

Climate indices are reliable tools for classifying climate and investigating aridity based on temperature and humidity (Pellicone et al., 2019). The De Martonne aridity index (I_{DM}; De Martonne, 1926) is one of the oldest and most widely used indices. Its simplicity of calculation makes it accessible and applicable in different geographical environments (except at the poles where temperatures have negative values), and it also facilitates the delimitation of climatic zones (Vlăduţ and Licurici, 2020; Ullah et al., 2022). Although there are other indices (UNEP index, Emberger index, Pinna Combinative Aridity index), the I_{DM} has shown good results in identifying and classifying regions based on their dry/humid conditions (Pellicone et al., 2019; Derdous et al., 2020; Jafarpour et al., 2023). For example, Troyo-Diéguez et al. (2014) evaluated the aridity conditions of northwest Mexico and noted that I_{DM} is a very useful tool for decision-making.

In short, climate change has led to significant changes in hydrological dynamics worldwide. Arid lands are among the places most susceptible to these changes. Many authors mention that dry lands will increase their territory in the future. Some studies have addressed the potential impacts of climate change on the NRB (Cerano-Paredes et al., 2011, 2012; González-Barrios et al., 2011; López-Santos et al., 2013; López-Santos and Martínez-Santiago, 2015; Ezquivel-Arriaga et al., 2017; Galloza et al., 2017). Yet, most of these investigations are limited to specific subregions or particular variables, and consequently, do not provide an integrated or comprehensive assessment of the basin as a whole.

Therefore, we hypothesize that the NRB will experience an increase in the extent of its most arid areas in the near and medium-term future due to CC. For this reason, the objective of this study was to evaluate the possible impact of CC on the extent and distribution of aridity in the NRB. This was achieved by comparing four CC models, previously used in studies in Mexico (Monterroso-Rivas and Gómez-Díaz, 2021; Ríos-Romero et al., 2024), with two shared socioeconomic trajectories and two time horizons: short-term (2021-2040) and medium-term (2041-2060). Additionally, we compared changes in land use and vegetation cover in the basin area, using maps generated by the Mexican government.

2. Brief description of study area

Mexico has 735 basins organized in 37 hydrological regions. The NRB is part of Hydrological Region 36 (HR-36), which is located in northern Mexico, inside the domain of the Tropic of Cancer line (23.5º N) (Fig. 1a). The climate of the NRB varies from subhumid to very arid, which is described as follows (CONABIO 2001): in the upper part of the basin, the climate is semi-cold, subhumid with long and cool summers, with average temperatures ranging between 5 and 12 ºC, and rain during the summer (Cb'[w2] Köppen Climate Classification System modified for Mexico by García [2004]). The middle part of the basin has a climate ranging from temperate semiarid (BS1kw) to warm semiarid (BSohw). The lower part of the basin has a very arid, semi-warm climate, with average temperatures ranging from 18 to 22 ºC and summer rain (BWhw) (Fig. 1b).

NRB is an endorheic hydraulic system (a condition in which the surface water drainage is landlocked; Wang, 2020) in an area of ~ 48 790 km². The Ramos and Sextín rivers originate in the Sierra Madre Occidental and descend to the Lázaro Cárdenas dam (Mojica-Guerrero et al., 2009) located at 25.587º N and 105.042º W, around 1650 masl. The Nazas River derives from the Lázaro Cárdenas dam. It is the longest river in the state of Durango and one of the most important in northern Mexico (Pinto et al., 2012), extending approximately 600 km to the region known as Comarca Lagunera (CL) at 1100 masl (Fig. 1c).

The CL is a region located in north-central Mexico, within the biogeographic region known as the Chihuahuan Desert, at the convergence of the states of Coahuila and Durango. The region has achieved considerable social and economic development despite the environmental conditions. As previously mentioned, the CL progress is due to the presence of the Nazas River and its aquifers, which allow the cultivation of its lands (Salas-Quintanal, 2011).

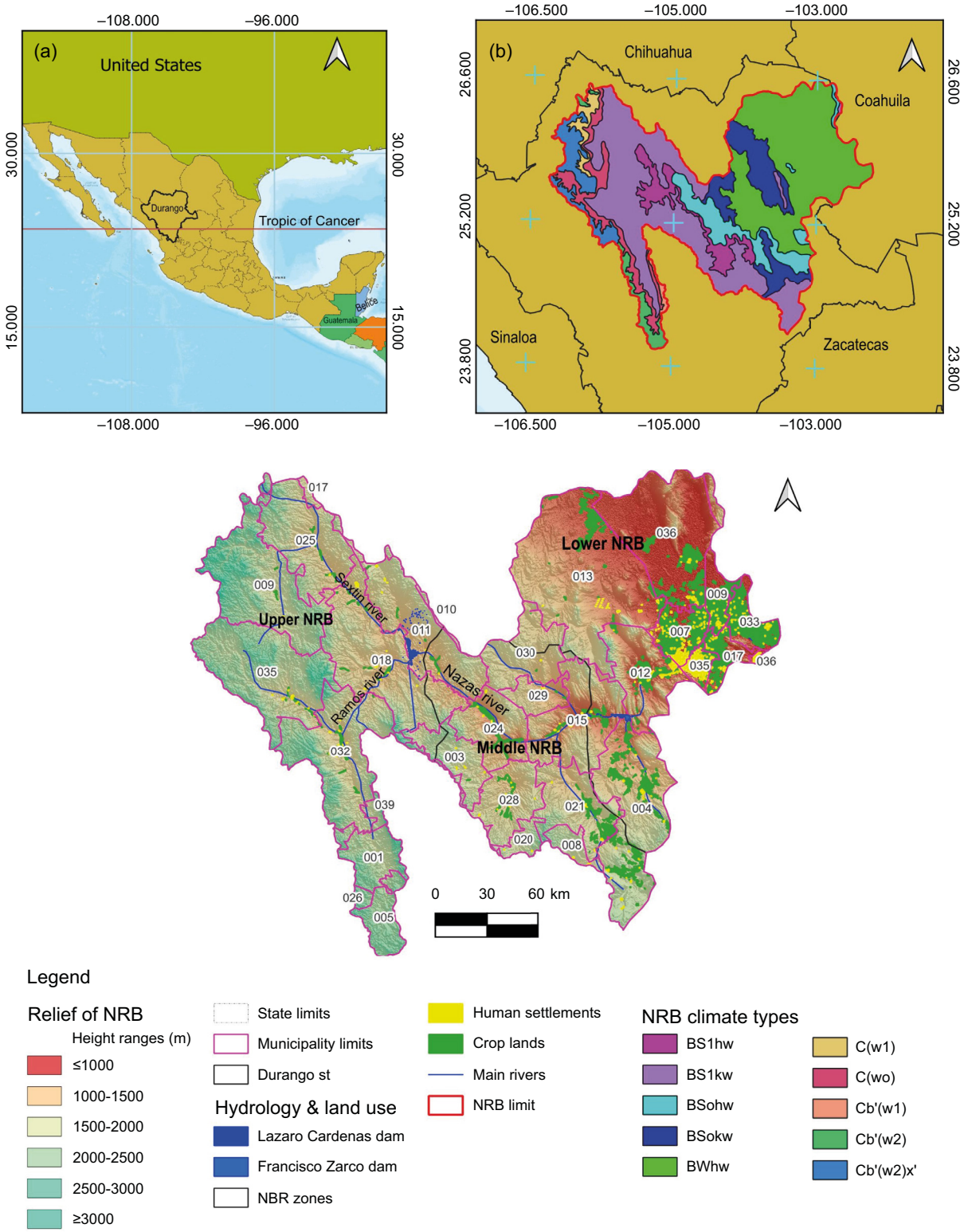

Fig 1. Nazas River basin (NRB) (between 26.325º N and 105.950º W; 26.578º N and 103.346º W; 24.016º N and 105.213º W; and 25.563º N and 103.093º W) references: (a) Mexico's political division and location of Durango; (b) NRB limits and climate distribution; (c) other important traits in the NRB, such as relief, main rivers, water reservoirs, rainfed croplands, human settlements, and municipality limits.

Currently, this region is Mexico's most important dairy basin, a center of manufacturing and agriculture. However, the environmental costs have led to the degradation of both the quality and quantity of basic natural resources (Cervantes and Franco, 2007) and the ecosystem services of the NRB. Therefore, it is worth highlighting what Correa-Islas et al. (2023) mentioned about the importance of knowing environmental dynamics with a CC perspective (Fig. 1c).

The CL is a young metropolitan area with great growth in recent years and is of great economic importance. The main use of water from the NRB is for agriculture, but it is controlled by two large dams, Lázaro Cárdenas and Francisco Zarco (25.268º and 103.778º), that have the capacity to retain approximately 438 million m^3 (Pedroza-González, 2011). The NRB is composed of 31 municipalities: 83.87% (26/31) are from Durango, and 16.13% (5/31) are from Coahuila (see Table SI in the supplementary material). Of these, 15 are part of the CL, where the water system is of vital importance for life (Fig. 1c).

3. Data and methods

3.1 Definition of the Nazas River basin's data source

The National Commission for the Knowledge and Use of Biodiversity (CONABIO, for its Spanish acronym) provides vector outline maps for all of Mexico's hydrological basins (CONABIO, 2023), which were legally established by the Federal Government by the end of the 2010s (SEMARNAT, 2018). Hydrological regions are subdivided into regions, basins, and sub-basins. The NRB, along with the Aguanaval river basin, comprises the RH-36 basin, also known as the Nazas-Aguanaval basin. The NRB was separated from the RH-36 basin due to its great importance to the project "Agua saludable para La Laguna" (healthy water for the La Laguna region), which is being carried out by the Mexican federal government, as well as for current and future ecology and restoration research studies.

3.2 Source and characteristics of the climate change models

We used data from four models obtained from WorldClim (2023) in raster format (spatial resolution of 2.5' × 2.5'), designed by Eyring et al (2016). The spatial resolution corresponds to 21.3 km^2, which covers the average extension of rainfed farms in northern Mexico.

The models used in this study, the Canadian Earth System Model (CanESM5), the National Centre for Meteorological Research model (CNRM-CM6-1), the HadGEM3-GC31-LL model from the Hadley Centre of the Meteorological Office, and the Model for Interdisciplinary Research on Climate (MIROC6), are part of the Coupled Model Intercomparison Project phase 6 (CIMP6). These are the most recent climate simulation models used to prepare the sixth IPCC (2021) assessment report.

Although all are widely used models (Swart et al., 2019; Gobie et al., 2024), CANESM5, CNRM-CM6-1, HADGEM3-GC31-LL, and MIROC6 have limitations such as low resolution, biases in precipitation and temperature, and difficulties in simulating climate extremes (Tatebe et al., 2019; Voldoire et al., 2019; Jones et al., 2024; Ríos-Romero et al., 2024). However, they offer significant advantages: CANESM5 allows large data ensembles (Swart et al., 2019), CNRM-CM6-1 improves vertical coupling (Voldoire et al., 2019), HADGEM3-GC31-LL accurately represents aerosols (Williams et al., 2018), and MIROC6 improved the ENSO and tropical circulation simulations (Tatebe et al., 2019). These capabilities strengthen the assessment of regional impacts and future climate projections. Because of this, using multiple models helps to better understand the potential impacts of climate change (Oo et al., 2019; Cui et al., 2025) on the NRB.

3.2.1 Brief model descriptions

3.2.1.1 CanESM5

This model includes updates to the atmospheric dynamics and the Earth's surface, as well as new components in the simulation of the oceans and sea ice. In addition, it incorporates coupler components that improve the interaction and interdependence between the modules (Swart et al., 2019). One of the relevant aspects of this model for the Mexican mesoclimate is that its evaluation includes the behavior of ENSO (El Niño-Southern Oscillation), which involves the oscillation of equatorial Pacific parameters and presents two well-known opposite phases: El Niño and La Niña (Swart et al., 2019).

3.2.1.2 HadGEM3-GC31-LL

It comprises models of atmosphere, ocean, sea ice, and land. Coupling between models uses the OASIS-MCT coupler. It is available in two atmosphere/ocean resolutions used for the historical simulations N96/ORCA1 or GC31-LL, and N216/ORCA025 or GC31-MM. Only the GC31-LL resolution is available in the WorldClim host. This configuration has an atmospheric resolution of 135 km (N96) and an oceanic resolution of 1º, with coupling every 3 h. The atmosphere model has 85 levels (up to 85 km), and the ocean model has 75 levels (Andrews et al., 2020).

3.2.1.3 CNRM-CM6-1

This model had important updates in the atmospheric and land surface components (Voldoire et al., 2019). For the atmospheric component, the changes were in the representation of the processes of superficial and deep convection, microphysics, and turbulence. On the land surface, snow and soil schemes were improved. In addition, the way of representing floods of rivers and aquifers was improved. The authors mention that calibrating this model was a significant challenge in achieving concrete results.

3.2.1.4 MIROC6

It is a numerical model that describes the global atmosphere in a three-dimensional way. The main updates on this model were made to the atmospheric component. Ocean and land surface components were updated in the horizontal coordinate system and had their vertical resolution increased. In addition, the cloud microphysics parameters were adjusted to ensure that the estimated radiative forcing was closer to the Fifth Assessment Report of the IPCC's best estimate. In general, simulations are better than their predecessor MIROC5 (Tatebe et al., 2019).

3.2.2 Baseline

The historical climate data and two shared socioeconomic pathways and their distinctive radiative forcings (SSP1-2.6 W m^{-2} and SSP5-8.5 W m^{-2}) and two time periods (2021-2040 and 2041-2060) of each model were selected (Fig. 2). The historical climate data is the 31-year baseline (1970-2000) and was released in January 2020. SSP1 (2.6 W m^{-2}) represents a scenario where rigorous policies were applied to reduce GHG emissions, while SSP5 (8.5 W m^{-2}) represents a scenario where development occurs based on fossil fuels and with lax climate policies.

3.3 Tools for the GIS process

The processing and editing of the shape and raster files were performed with the open-source software Qgis (3.22.11 Biatowieza). First, we delimited the study area, for which we downloaded the shape file of the hydrological basins of Mexico from CONABIO (2023) and selected the polygons that correspond to the NRB. We extracted this area to use as our main mask. Later, we performed the cuts and extractions using the mask layer with the other input files.

3.4 Analysis criteria of climate change impacts

To analyze the extent of arid land expansion that may occur in the NRB, we used the I_{DM} (Eq. 1), which was estimated with the 31-year historical bioclimatic variables (1970-2000) and in two shared socioeconomic pathways (SSP1-2.6 W m^{-2} and SSP5-8.5 W m^{-2}) in the two time periods (2021-2040 and 2041-2060) of each model.

$$I_{DM} = \frac{P}{T + 10} \quad (1)$$

where I_{DM} is the De Martonne's aridity index (1926), P is the mean annual precipitation in mm, T is the annual mean temperature in ºC, and 10 is a constant value used to avoid negative values. The ranges of I_{DM} values can delimit six climatic zones, as shown in Table I, which were used previously by López-Santos et al. (2013), Troyo-Diéguez et al. (2014), and López-Santos and Martínez-Santiago (2015).

Once the 17 raster files were obtained (historical I_{DM}, SSP1 2.6 W m^{-2} I_{DM} [2021-2040], SSP1-2.6 W m^{-2} I_{DM} [2041-2060], SSP5-8.5 W m^{-2} I_{DM} [2021-2040], and SSP5-8.5 W m^{-2} I_{DM} [2041-2060] of the selected models), each was reclassified to yield integer pixel values and was transformed into shape files (Fig. 2).

We established the categories of the aridity index and calculated the areas of each polygon with a field calculator. To reduce the number of polygons and eliminate those that did not meet the minimum mappable cell area of 15 × 15 km, which is closest to the raster resolution of the four models (2.5' spatial resolution). Then we used the "remove selected polygons" tool, and the selected polygons were combined with the larger adjacent area.

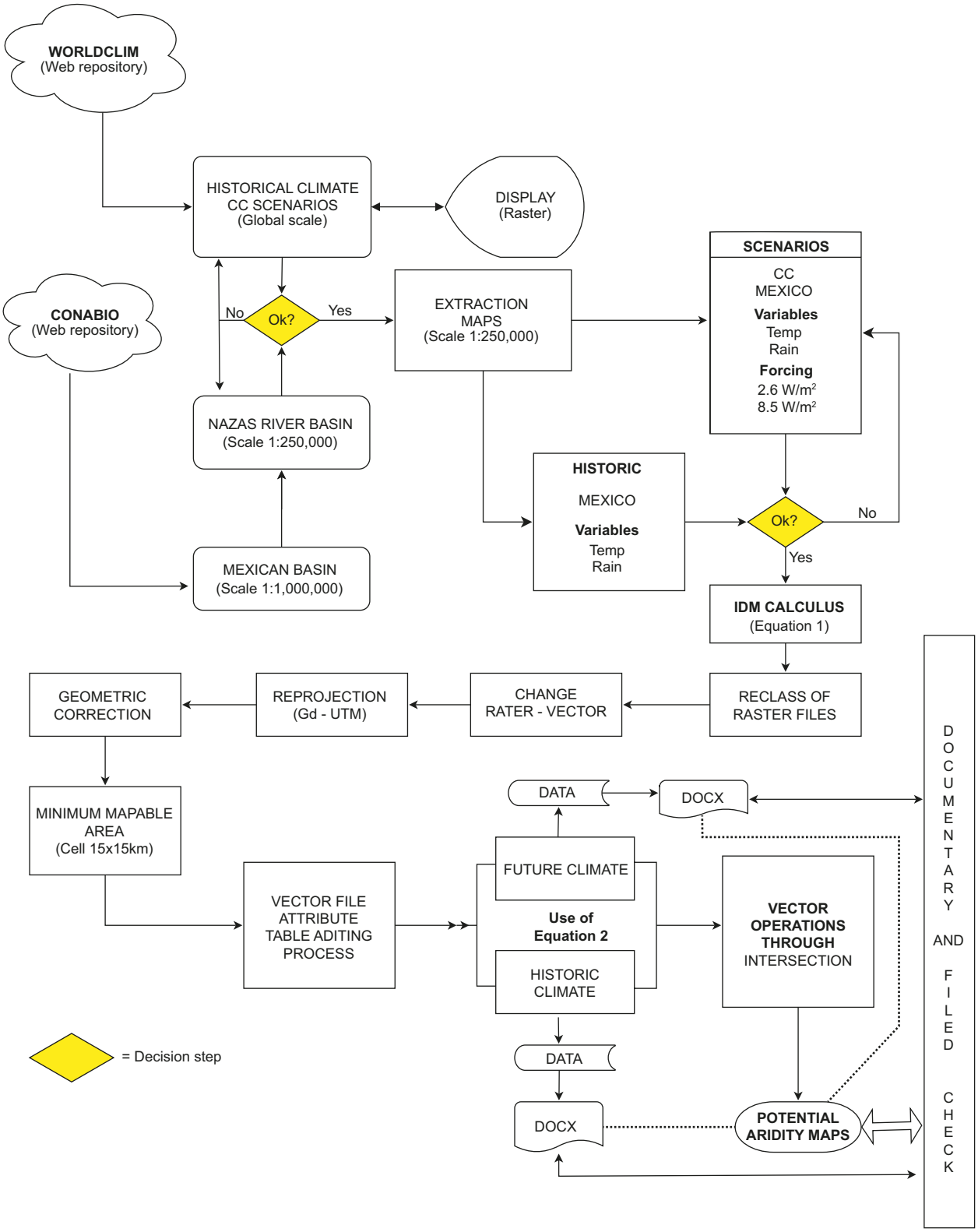

Fig. 2. Flux diagram to analyze and determine the geographical impact of climate change.

Table I. De Martonne's aridity index categories.

Category	Values
Hyper-arid	< 5.00
Semiarid	5.01-10.00
Mediterranean semiarid	10.01-20.00
Subhumid	20.01-30.00
Humid	30.01-60.00
Hyperhumid	> 60.01

Subsequently, in each scenario, the estimate of the area covered by each category of the aridity index was obtained with the "statistics by category" tool. The data obtained were exported and grouped in Microsoft Excel. We calculated the coverage percentages of each category in all scenarios. To assess whether changes in aridity were significant, multiple chi-square tests were performed. These tests compared the percentage composition of the aridity categories in the I_{DM} for each scenario with the percentage composition of the IDM categories using historical data.

All attribute tables were edited separately, and fields with numerical codes were added to each of the six I_{DM} types according to Table II. The vector files were then compared between historical and vector files for each scenario with significant differences in the chi-square tests, using the intersect tool in the GIS process in accordance with the guidance on good practices in the evaluation of changes in land use and land cover proposed by the IPCC (1996, 2014), recently used by Bueno-Hurtado et al. (2017). The geographic intersection represented can be identified in the attribute table based on the design of the change chart shown in Table SII in the supplementary material.

Next, the intensity of the climatic change impact (Eq. 2) was calculated as the sum of all changes or those that did not change (remained) in the NRB as shown next:

$$ICCI = \frac{\Sigma(C1_{xi} + C2_{yi})}{TS_{NRB}} \times 100 \quad (2)$$

where $ICCI$ could be zero or more than zero; $C1_{xi}$ and $C2_{y2}$ are the sum of all surfaces regarding the numerical codes defined (Table II), and TS_{NRB} is the total surface of the NRB. The codes in the diagonal line of Table II represent zero impact.

3.5 Analysis of land use and vegetation cover

We downloaded the land use and vegetation cover (LUVC) maps, series three (2003) and seven (2018) from the CONABIO repository (reviewed in 2023). For this, we again extracted the study area from both maps. To observe the changes in the NRB, we first standardized the categories used by the National Institute of Statistics and Geography (INEGI, for its Spanish acronym) according to the IPCC (2019), which proposes six general categories that are the basis for estimating and reporting GHG emissions and removals from land use and land use conversions.

These categories are broad enough to classify all land areas in most countries and to accommodate differences in national land use classification systems.

Table II. Basis for editing the attribute tables for the spatial analysis of climate change's impact.

		T2. Future scenario					
		Hyperarid	Semiarid	Mediterranean semiarid	Subhumid	Humid	Hyperhumid
		Code 2 and sum					
T1. Historic	Code 1	100	200	300	400	500	600
Hyper-arid	10	**110**	210	310	410	510	610
Semiarid	20	120	**220**	320	420	520	620
Mediterranean Semiarid	30	130	230	**330**	430	530	630
Subhumid	40	140	240	340	**440**	540	640
Humid	50	150	250	350	450	**550**	650
Hyper-humid	60	160	260	360	460	560	**660**

Code 1, and Code 2, arbitrary values assigned for the matrix generation; sum: Code 1 + Code 2 for each intersection; diagonal lines in bold represent unchanged situations.

The six categories are: forest land (FL), cropland (CL), grassland (GL), wetlands (WL), settlements (S), and other land (OL, which, according to the IPCC [2019], includes bare soil, rock, ice, and all land areas that do not fall into any of the other five categories). Then we overlapped both maps from series three and series seven and made a transition map with the "intercept" tool. Finally, we performed a transition matrix of LUVC and a LUVC change rate. To calculate the change rate, we used Eq. (3) (FAO, 1996).

$$\delta = \left(\frac{S_2}{S_1}\right)^{\frac{1}{n}} - 1 \tag{3}$$

where δ is the annual change rate, S_1 is the LUVC in time 1 (series three), S_2 is the LUVC in time 2 (series seven), and n is the difference in years between time 1 and time 2.

4. Results

4.1 Historical De Martonne Index

The zoning in the NRB based on historical data from 31 years (1970-2000) with the IDM, indicates a predominance of Mediterranean semiarid climate (44%) in the middle part of the basin, followed by semiarid climate (20%) in the lower part. The subhumid (24%) and humid (12%) classifications occur in the upper part of the basin. This shows that 64% (30 348.8 km^2) of the NRB has some degree of aridity (Fig. 3).

4.2 Analysis of territorial future impacts

The comparisons of the I_{DM} categories percentages are shown in Table III. Almost all models show an increasing trend in arid zones (1-7% in semiarid and 1-10% in Mediterranean semiarid) and a decreasing trend in humid zones (both subhumid and humid). Interestingly, only the CNRM-CM6-1 model in SSP1-2.6 W m^{-2} for 2041-2060, and SSP5-8.5 W m^{-2} for 2021-2040 and 2041-2060, show significant differences with respect to the I_{DM} with historical data. Furthermore, the CNRM-CM6-1 model in the SSP1 2041-2060 and SSP5 2021-2040 scenarios were similar to each other.

I_{DM} with the CNRM-CM6-1 model in the SSP1-2.6 W m^{-2} for the period 2041-2060 and SSP5-8.5 W m^{-2} for the period 2021-2040 were similar in both areas and percentages (Table III). Both showed a strong expansion of the Mediterranean semiarid category and a decrease in the humid and subhumid categories towards the upper part of the basin (Figs. 4 and 5) compared with the historical I_{DM}. The Mediterranean semiarid category increased from 44 to 54% coverage (Table III), and the semiarid category increased from 20 to 24% coverage in these scenarios. The total aridity of the basin increased 14% (from 64 to 78%).

The greatest increase in aridity within the NRB occurred with the CNRM-CM6-1 in the SSP5 8.5 W m^{-2} scenario for the period 2041-2060. It is observed how the arid zones move strongly towards the upper part of the basin, and the more humid zones continue to contract drastically (Fig. 6). In this scenario, the arid zones increase from 64% (20% in historical semiarid and 44% in Mediterranean semiarid) to 81% (27% in semiarid and 54% in Mediterranean semiarid). Interestingly, the Mediterranean semiarid category (54%) remained similar with respect to the scenarios mentioned above (Fig. 4), while the semiarid category only increased by 3% (from 24 to 27%).

4.3 Land use and land cover changes

The most obvious anthropogenic impacts are seen in land use and vegetation cover changes. From 2003 to 2018 (Fig. 7), most of the territory on the banks of the river has undergone changes in land use, primarily as grasslands in the upper part of the basin and croplands in the lower part. However, the rates of change and the transition matrix show that some of these grasslands were transformed into croplands and wetlands (Tables IV and V).

On the other hand, in the lower part of the basin, a notable increase in human settlements is observed. The largest settlements in this area are the three most populated and industrialized cities in the Comarca Lagunera: Torreón, Gómez Palacio, and Lerdo. The expansions of the settlements were established in areas with cultivated lands. However, over these 15 years, the deterioration of the basin's territory has been statistically non-significant (Tables IV and V). Although the rate of change and the territory occupied by settlements are not significant, the overall impact has more than doubled throughout the basin.

5. Discussion

The most relevant results are the following: the NRB is predominantly arid (20% semiarid and 44%

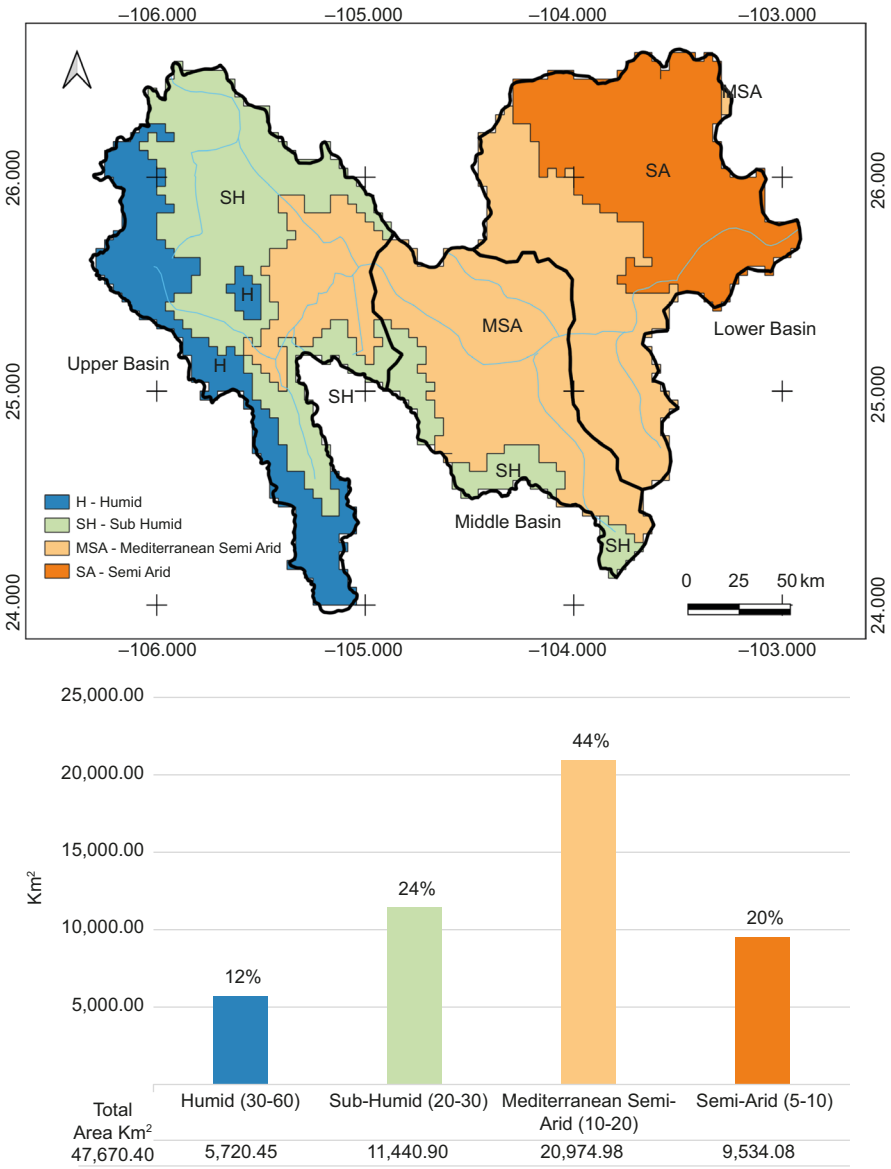

Fig. 3. De Martonne's aridity index with historical data in the Nazas river basin. Baseline of data: 31 years (1970-2000). (H: humid; SH: subhumid; MSA: Mediterranean semiarid; SA: semiarid.)

Mediterranean semiarid) according to the I_{DM} with historical data (Fig. 3). Most of the climate change models analyzed in this study show that with either of the two socioeconomic trajectories, aridity within the basin would increase (Table III); however, they are not significant according to the chi square test for the proportions of the territory. Only the CNRM-CM6-1 model in SSP1 (2041-2060) and SSP5 in both periods show significant proportional changes. The CNRM-CM6-1 SSP5 model (2041-2060) shows that the aridity of the NRB could increase by up to 81%. Finally, the analyses of land use change and vegetation cover show no statistically significant changes; however, a trend (albeit low) towards an increase in human settlements, wetlands, and croplands is observed.

Table III. Chi-square comparison of percentages of De Martonne's aridity index (I_{DM}) categories between models and scenarios.

Model	Total basin area 47,670.40 Km^2	SSP1 2021-2040		SSP1 2041-2060		SSP5 2021-2040		SSP5 2041-2060	
CanESM5	Zone	IR%	Test statistics	IR%	Test statistics	IR%	Test statistics	IR%	Test statistics
	Semiarid (5-10)	20%	$X^2 = 0.0$	21%	$X^2 = 0.64$	21%	$X^2 = 0.64$	23%	$X^2 = 4.355$
	Mediterranean semiarid (10-20)	44%	df = 3	45%	df = 3	45%	df = 3	51%	df = 3
	Subhumid (20-30)	24%	$p = 1.0$	23%	$p = 0.996$	23%	$p = 0.996$	17%	$p = 0.226$
	Humid (30-60)	12%		12%		11%		9%	
CNRM-CM6-1	Zone	IR%	Test statistics	IR%	Test statistics	IR%	Test statistics	IR%	Test statistics
	Semiarid (5-10)	24%	$X^2 = 7.234$	**24%**	$X^2 = 8.573$	**24%**	$X^2 = 8.573$	**27%**	$X^2 = 12.76$
	Mediterranean Semiarid (10-20)	52%	df = 3	**54%**	df = 3	**54%**	df = 3	**54%**	df = 3
	Subhumid (20-30)	14%	$p = 0.065$	**14%**	$p = 0.036$	**14%**	$p = 0.036$	**13%**	$p = 0.005$
	Humid (30-60)	9%		**8%**		**8%**		**6%**	
HadGEM3-GC31-LL	Zone	IR%	Test Stats	IR%	Test Stats	IR%	Test Stats	IR%	Test Stats
	Semiarid (5-10)	19%	$X^2 = 0.105$	23%	$X^2 = 1.78$	21%	$X^2 = 0.239$	23%	$X^2 = 2.04$
	Mediterranean Semiarid (10-20)	45%	df = 3	47%	df = 3	45%	df = 3	47%	df = 3
	Subhumid (20-30)	23%	$p = 0.991$	19%	$p = 0.619$	22%	$p = 0.971$	19%	$p = 0.564$
	Humid (30-60)	12%		11%		12%		10%	
MIROC6	Zone	IR%	Test statistics	IR%	Test statistics	IR%	Test statistics	IR%	Test statistics
	Semiarid (5-10)	22%	$X^2 = 1.041$	23%	$X^2 = 1.78$	23%	$X^2 = 1.78$	24%	$X^2 = 4.41$
	Mediterranean Semiarid (10-20)	46%	df = 3	47%	df = 3	47%	df = 3	50%	df = 3
	Subhumid (20-30)	20%	$p = 0.79$	19%	$p = 0.619$	19%	$p = 0.619$	17%	$p = 0.22$
	Humid (30-60)	11%		11%		11%		9%	

SSP1: radiative forcing of 2.6 W m^{-2}; SSP5: radiative forcing of 8.5 WW m^{-2}. Percentages in bold represent significant differences with respect to the historical I_{DM}.

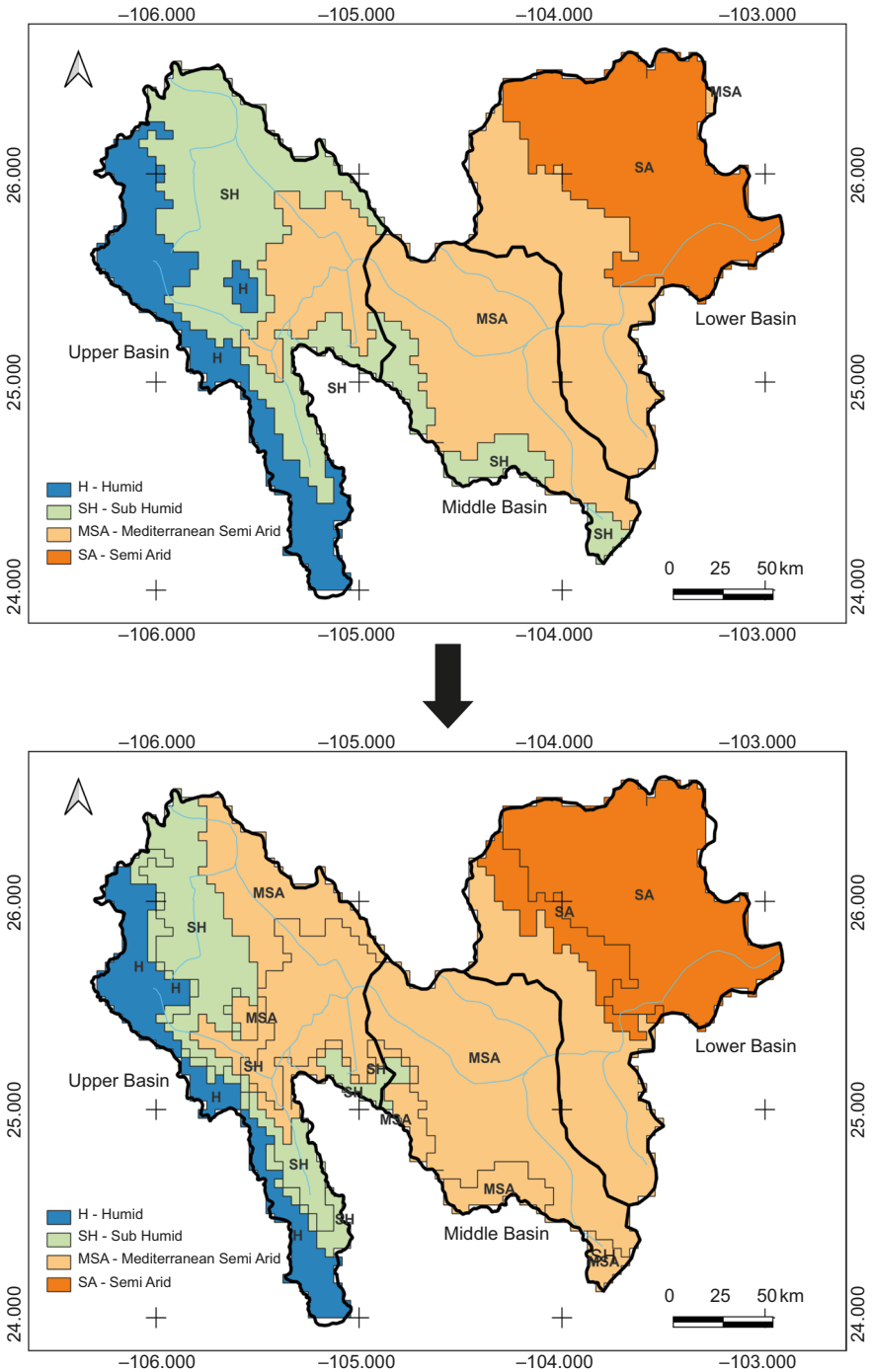

Fig. 4. Transition from the historical I_{DM} (left panel) to the I_{DM} with the CNRM-CM6-1 model in the SSP1-2.6 W m^{-2} scenario (2041-2060) (right panel) in the Nazas River basin. (H: humid; SH: subhumid; MSA: Mediterranean semiarid; SA: semiarid.)

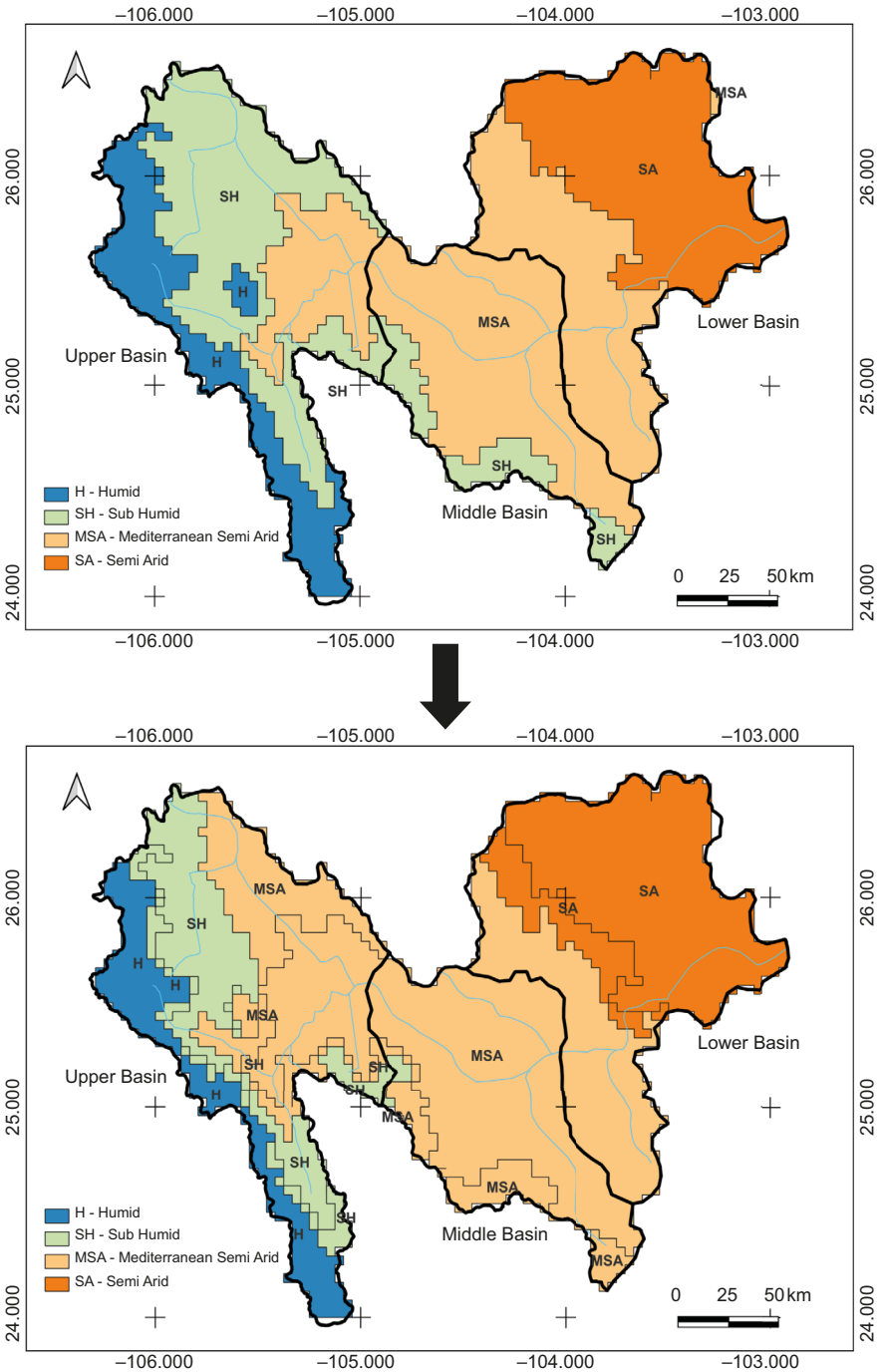

Fig. 5. Transition from the historical I_{DM} (left panel) to the I_{DM} with the CNRM-CM6-1 model in the SSP5-8.5 W m^{-2} scenario (2021-2040) (right panel) in the Nazas River basin. (H: humid; SH: subhumid; MSA: Mediterranean semiarid; SA: semiarid.)

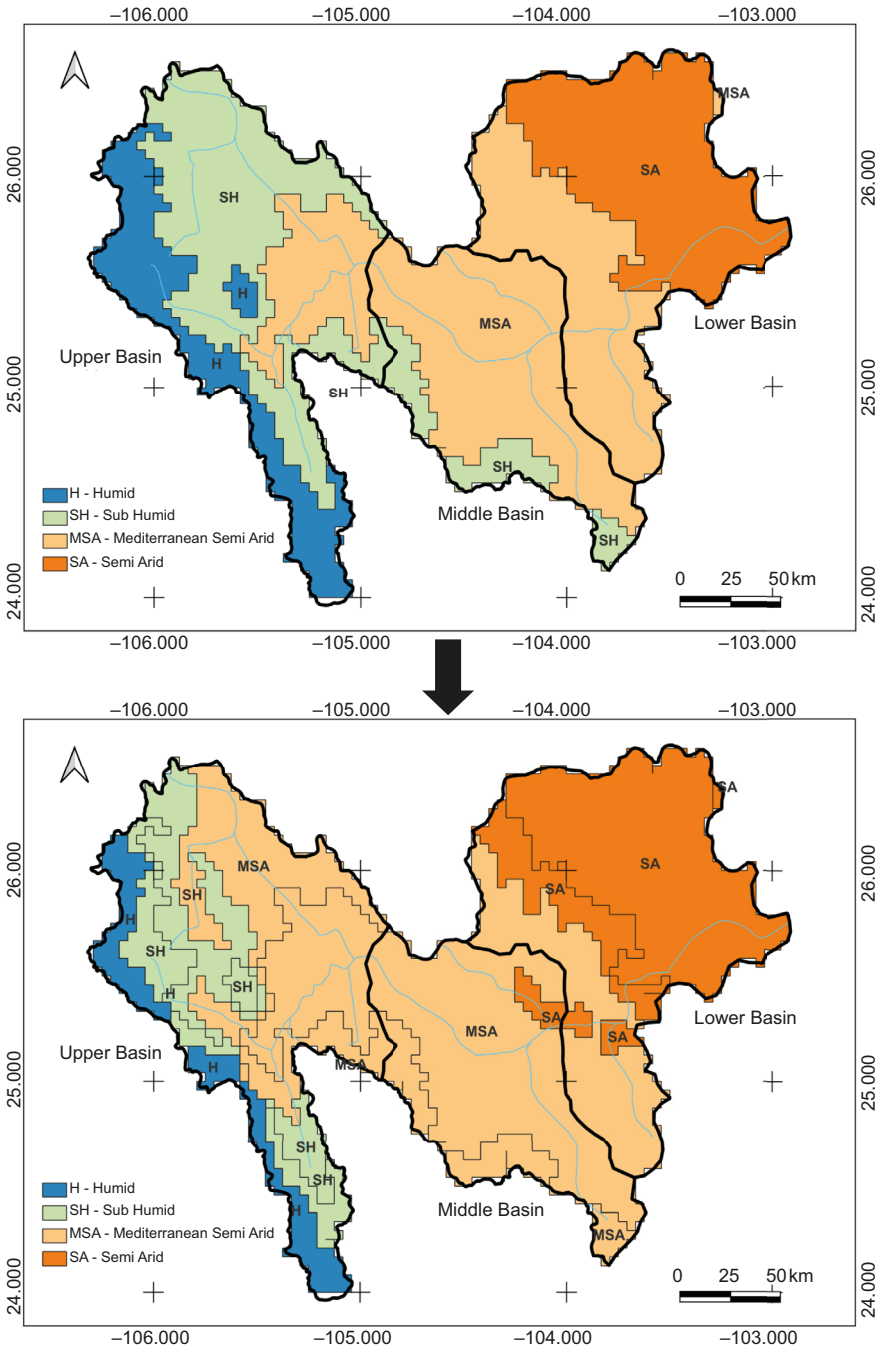

Fig. 6. Transition from the historical I_{DM} (left panel) to the I_{DM} with the CNRM-CM6-1 model in the SSP-8.5 W m^{-2} scenario (2041-2060) (right panel) in the Nazas River basin. (H: humid; SH: subhumid; MSA: Mediterranean semiarid; SA: semiarid.)

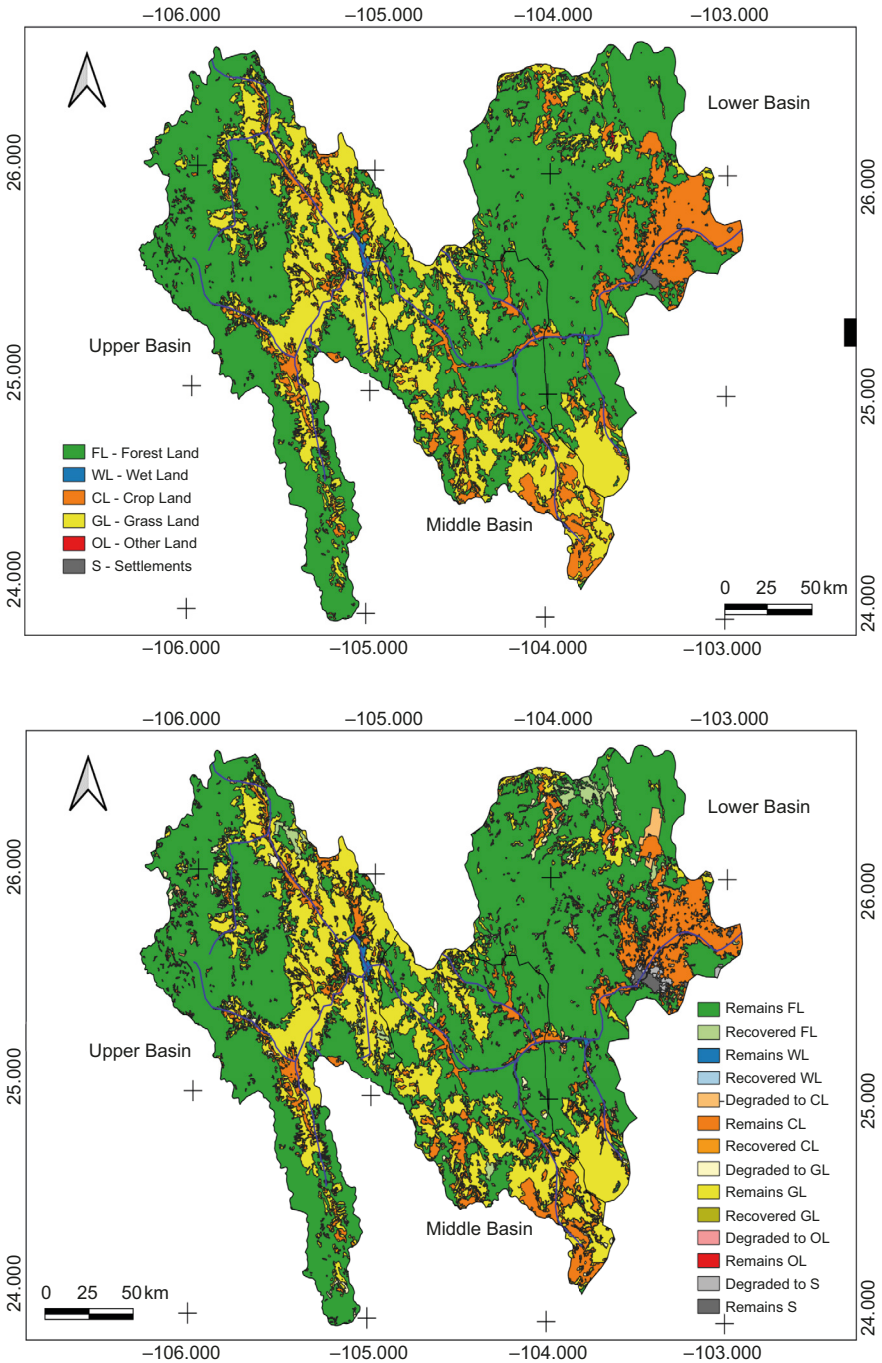

Fig. 7. Land use and vegetation cover map in 2003 (series 3, left panel) and changes to 2018 (series 7, right panel).

Table IV. Land use and land vegetation cover changes from 2003 (LUVC-S3) to 2018 (LUVC-S7).

Category	LUVC-S3 2003 (km^2)	LUVC-S7 2018 (km^2)	Change rate (%)	2003 (%)	2018 (%)	Statistics
FL	29,584.49	29,409.12	–0.040	60.64	60.28	$X^2 = 0.115$
WL	145.87	159.58	0.601	0.30	0.33	$df = 2$
CL	6,445.32	6,589.33	0.147	13.21	13.51	$p = 0.944$
GL	12,373.11	12,113.34	–0.141	25.36	24.83	
OL	68.71	64.4	–0.431	0.14	0.13	
S	172.59	454.32	6.665	0.35	0.93	

LUVC: land use and vegetation cover; FL: forest land; WL: wetlands; CL: cropland; GL: grassland; OL: other land; S: settlements.
The chi-square test was applied to compare changes between the LUVC-S3 and LUVC-S7 percentages.

Table V. Land use and vegetation cover transition matrix between 2003 and 2018.

		LUVC-S7 (2018)					
		FL	WL	CL	GL	OL	S
		Code 2 and surface in km^2					
LUVC-S3 (2003)	Code1	10	20	30	40	50	60
FL	1	**28505.37**	11.942	542.41	420.58	19.16	85.03
WL	2	0.88	**123.754**	9.19	1.11	6.97	3.96
CL	3	301.43	11.052	**5761.47**	185.91	3.13	182.33
GL	4	583.13	12.786	256.61	**11502.81**	5.78	12
OL	5	17.26	0	17.21	2.91	**29.29**	2.03
S	6	1.05	0.051	2.44	0.01	0.07	**168.97**

LUVC: land use and vegetation cover; FL: forest land; WL: wetlands; CL: cropland; GL: grassland; OL: other land; S: settlements. Numbers in bold represent areas that remain unchanged in land use between both periods.

5.1 Signals of the climate change impact on a local level

Most of the models used in this study showed a tendency toward the expansion of arid zones. The Mediterranean semiarid category shifted slightly from the lower to the upper part of the basin, while the semiarid category expanded in the lower part. The expansion of arid zones is a phenomenon supported by several authors (Seager et al., 2009; Zhang et al., 2024), who mention that the modeling of climate scenarios suggests an increase in aridity at global and regional levels (López-Santos et al., 2013; López-Santos and Martínez-Santiago, 2015; Neri and Magaña, 2016; Galloza et al., 2017; Murray-Tortarolo et al., 2018; Monterroso-Rivas and Gómez-Díaz, 2021; Ríos-Romero et al., 2024).

Despite the changes, we did not find hyperarid zones, not even with the CNRM-CM6-1 model, which presented the most significant changes (Figs. 4, 5, and 6). However, the Durango State Action Program on Climate Change (Pinto et al., 2012) mentions that this area could be affected by increases in maximum temperatures, reaching 53.9 ºC over a long period of time (2060-2090) within the A2 scenario (continuous population growth). This agrees with López-Santos et al. (2013), who mention that the municipality of Gómez Palacio, Durango (located in the lower part of the NRB) is susceptible to becoming hyperarid in 13 072 hectares (15%) of the municipal territory, due to exposure characterized by orographic, topographic, and microclimatic conditions. Interestingly, Zhang et al. (2024) argue that

despite increasing climatic aridity, arid ecosystems could be sustained.

Our results show that the areas most affected by the increase in aridity are mainly in the upper part of the basin. In contrast, Ezquivel-Arriaga et al. (2017) highlighted increases in precipitation, runoff, and temperature averages (1 ºC maximum and minimum temperature) in the meteorological stations of the upper part of the basin near the Sextín river with scenarios A1B (rapid economic growth) and A2 in two time intervals (2010-2039 and 2040-2069). In addition, Cerano-Paredes et al. (2011) mention that precipitation in the upper part of NRB is regulated by ENSO, which causes severe droughts during the cold stage (La Niña) and significantly increases precipitation during the warm stage (El Niño). This suggests that there may be specific effects at smaller scales, so a combination of point and large-scale studies is needed.

5.2 Signals of the intensification of human radiative forcing

Changes in land use and vegetation cover towards more anthropogenic uses are the most significant drivers of an ecosystem's health (Xi et al., 2023; Zhang et al., 2024). In the NRB area, there is a trend (statistically not significant) towards land degradation, transforming forest lands into productive lands, mainly croplands, and croplands into human settlements in the lower part of the basin (Fig. 7; Tables IV and V).

Over the past 15 years, human settlements have experienced an annual growth rate of 6.66% in the NRB area, which is comparable with the study by Rimal et al. (2018), where the cities of the Kathmandu Valley grew by around 9.15%, and the study by Zhang et al. (2024), where the metropolitan area of Shanghai grew by 10.38% annually. Although human settlements cover a proportionally small area of the NRB, Zhang et al. (2024) mention that these areas are the most influential drivers of global warming and climate change. This could be because these small areas concentrate GHG production, increase the heat island effect, and generate the most drastic changes in land use by eliminating vegetation cover and water bodies, and creating impervious surfaces.

In the lower part of the basin, the possibly affected areas on the banks of the river are within the protected natural area "Cañón de Fernández". There, forest lands, and some wetlands changed to farmlands and human settlements (Fig. 7 and Table IV). According to Kalnay and Cai (2003), croplands have a thermoregulatory effect that reduces the range of daily temperature variability as a result of irrigation, which increases the thermal capacity of the soil and the environment due to the water content in both.

Leija-Loredo et al. (2020) mention that during the period 1990-2016, the natural vegetation in the riverside area in Cañón de Fernández had been transformed for agricultural activity. In those 26 years, 4% of the gallery forest and 26% of the xerophytic scrubs in the state park were lost. In this study, the change in land use and vegetation cover occurred from 2003 to 2018 and did not show significant differences. This could mean that the most abrupt change in vegetation could have occurred sometime between 1990 and 2003. In any case, the loss of forest land affects the capacity to provide ecosystem services (Morales-Estrada, 2022). In addition, it could have direct consequences on the hydrodynamic processes of the basin, such as runoff, infiltration, deep percolation, water absorption by plants, and evapotranspiration (González-Barrios et al., 2011; Huo et al., 2013; Asadi et al., 2017).

On the other hand, most of the riverbank and a large part of the territory (24.8%) in the upper part of the basin is grassland, and this area is the one with the greatest tendency to increase aridity. In this regard, the history of the region suggests that there was an expansion of grasslands due to agricultural and livestock restructuring policies from 1955 onwards (Cerutti and Rivas-Sada, 2008). This means a reduction in forest lands, leaving the lands exposed to excessive overgrazing on the riverbank and more susceptible to erosion. This highlights the importance of having a restoration plan for forest lands in the upper part of the basin.

5.3 Signals of the combined effect or reversibility/ adaptation

Forest lands have a greater resilient capacity based on water production and erosion control (González-Barrios et al., 2011; IPCC, 2019). However, the remaining forest ecosystem may be threatened by increasing temperatures and droughts (Choat et al., 2018). The lack of information on the dynamics of climatic

variables, such as atmospheric humidity, leads to the affected area and forest vulnerability being underestimated (Allen et al., 2015).

Ecosystems have the capacity to withstand impacts, whether natural or anthropogenic, but this capacity is mainly determined by the rate of change when transitioning from one state to another in the future, and by the intensity of this change (Bastiaansen et al., 2020). However, the transformation towards uncontrolled productive systems (grasslands and crop lands) significantly affects these processes at the basin scale and intensifies the effects of climate change, especially in the upper part.

In the lower part of the basin, there is no increase in aridity according to the I_{DM} in the different models and shared socioeconomic pathways; however, the rate of increase in human settlements is greater than 6%, and even though they are small territories, they play a very important role in radiative forcing. This, along with inadequate management of human settlements and their expansion, increases the pressure on ecosystems, leading to their fragmentation and, consequently, the risk of environmental imbalance (Rimal et al., 2018).

On the other hand, there are no significant statistical differences in changes in land use and vegetation cover. In this sense, this would appear to represent a low intensification of human radiative forcing, implying that with good practices and public policies, dryland ecosystems could maintain their functions. Furthermore, as Bastiaansen et al. (2020) mention, small and gradual alterations in ecosystems can allow them to adapt and continue to function. This is consistent with Zhang et al. (2024), who mention that despite climate change, less than 4% of drylands would be affected by desertification.

The socio-ecosystemic diversity of the basin, along with its large number of heterogeneous components, non-linear interrelations, varied evolution, adaptability, self-organization, emergent properties, and shared administration by two Mexican states, makes the NRB a highly complex system. Because of this, interdisciplinary, detailed, and comprehensive studies are needed to understand the socio-ecosystemic functioning of the basin, as well as the possible threats and implications of climate change and its synergy with human activities. Therefore, this work serves as a basis for other relevant research projects and supports decision-making for the creation of sustainable development policies and programs to mitigate the effects of climate change.

6. Conclusions

The NRB is of vital importance for the economic and social development of the Comarca Lagunera. The effects of interactions between climate change and anthropogenic activity on the NRB socioecosystems are not well understood. That is why this work aimed to evaluate the possible areas of aridity change caused by climate change through cartographic analysis with the I_{DM}, using historical data and different climate change models, two shared socioeconomic pathways (2.6 and 8.5 W m^{-2}), and two periods (short and medium term). In addition, the anthropogenic disturbances were analyzed by comparing the change in land use and vegetation cover in the NRB.

This study shows that the NRB is arid in 64% of its surface. The assessment of the extent of aridity indicates an increase in the NRB using the four models, although only the CNRM-CM6-1 showed significant changes with the scenarios of 2.6 W m^{-2} (2041-2060) and 8.5 W m^{-2} (both periods). The category of greatest aridity was semiarid in the lower part of the basin, and there are no expectations that it will increase to hyperarid in the medium term. The change in aridity can occur in a shorter time with a radiative forcing of 8.5 W m^{-2} (2021-2040) compared to 2.6 W m^{-2} (2041-2060). The results suggest that 29% of the NRB could be threatened by increased aridity, mainly in the upper part of the basin, with the CNRM-CM6-1 8.5 W m^{-2} (2041-2060) scenario.

On the other hand, land use and vegetation cover have experienced non-significant changes from 2003 to 2018. However, during this period, human settlements grew at an annual rate of 6.6% (from 172.59 to 454.32 km^2). Although human settlements cover a very small surface area compared to the basin area (less than 1% in this study), the impact of human activities related to human settlements plays an important role in GHG generation and intensification of radiative forcing. Furthermore, productive land, primarily cropland, has increased. This could impact CO_2 retention, leading to greater susceptibility to erosion and changes in soil hydrodynamic processes. These changes increase the likelihood of

desertification, potentially generating increased radiative forcing and consequently intensifying the effects of climate change.

The results show a general picture in which climate change may cause no significant changes in aridity conditions and low land degradation. This is favorable for the stability and functioning of ecosystems in the NRB. The methods used (the I_{DM} combined with comparisons with climate change scenarios) can be a useful tool to support decision-making and the creation of sustainable development policies and programs that help mitigate the effects of climate change. However, we suggest conducting further studies when new updates to climate change models become available. Furthermore, due to the complexity of the NRC, comprehensive interdisciplinary studies are required to better understand the social ecosystem processes that make up the basin with a view to sustainable development, mitigation, and adaptation to climate change.

Acknowledgments

GJPU thanks SECIHTI for the scholarship awarded in the "Estancias posdoctorales por México 2022" call. He also thanks the Juárez University of the State of Durango for providing its facilities to carry out the research. We also thank Jorge Alejandro Torres González for his valuable collaboration in obtaining literature.

References

Allen CD, Breshears DD, McDowell NG. 2015. On underestimation of global vulnerability to tree mortality and forest die-off from hotter drought in the Anthropocene. Ecosphere 6: 129. https://doi.org/10.1890/ES15-00203.1

Andrews MB, Rifley JK, Wood RA, Andrews T, Blockley EW, Booth B, Burke E, Dittus AJ, Florek P, Gray LJ, Haddad S, Hardiman SC, Hermanson L, Hodson D, Hogan E, Jones GS, Knight JR, Kuhlbrodt T, Misios S, Mizielinski MS, Ringer MA, Robson J, Sutton RT. 2020. Historical simulations with HadGEM3-GC3.1 for CMIP6. Journal of Advances in Modeling Earth Systems 12: e2019MS001995. https://doi.org/10.1029/2019MS001995

Asadi Zarch, MA, Sivakumar B, Malekinezhad H, Sharma A. 2017. Future aridity under conditions of global climate change. Journal of Hydrology 554: 451-469, https://doi.org/10.1016/j.jhydrol.2017.08.043

Bastiaansen R, Doelman A, Eppinga MB, Reitkerk M. 2020. The effect of climate change on the resilience of ecosystems with adaptive spatial pattern formation. Ecology Letters 23: 414-429. https://doi.org/10.1111/ele.13449

Bueno-Hurtado P, López-Santos A, Sánchez-Cohen I, Velásquez-Valle MA, González-Barrios JL. 2015. Cambios de uso de suelo y sus efectos sobre la dinámica de GEI en el estado de Durango, México. Tecnología y Ciencias del Agua 6: 75-84.

Cerano-Paredes J, Villanueva-Díaz J, Valdez-Cepeda RD, Arreola-Ávila JG, Constante-García V. 2011. Effects of the El Niño Southern Oscillation on precipitation in the upper Nazas River watershed. Revista Chapingo Series Ciencias Forestales y del Ambiente 17: 207-215. https://doi.org/10.5154/r.rchscfa.2010.09.076

Cerano-Paredes J, Villanueva-Díaz J, Valdez-Cepeda RD, Constante-García V, González-Barrios JL, Estrada-Ávalos J. 2012. Reconstructed precipitation for the upper Nazas River Basin, Durango. Revista Mexicana de Ciencias Forestales 3: 7-23. https://doi.org/10.29298/rmcf.v3i10.525

Cerutti M, Rivas-Sada E. 2008. La construcción de la cuenca lechera en La Laguna (1948-1975). Estudios Sociales 16: 165-204.

Cervantes RMC, Franco González AM. 2007. Diagnóstico ambiental de La Comarca Lagunera. In: Foro Interdisciplinario sobre la Comarca Lagunera (López López Á y Carmona Mares R, Eds.). Sociedad Mexicana de Geografía y Estadística, Mexico City. Available at: https://es.scribd.com/document/399713983/Diagnostico-Ambiental-de-La-Comarca-Lagunera (accessed on August 20, 2025)

Cherlet M, Hutchinson C, Reynolds J, Hill J, Sommer S, von Maltitz G, eds. 2018. World Atlas of Desertification. Publication Office of the European Union, Luxembourg. Available at: https://wad.jrc.ec.europa.eu/ (accessed on October 21, 2021).

Choat B, Brodribb TJ, Brodersen CR, Duursma RA, López R, Medlyn BE. 2018. Triggers of tree mortality under drought. Nature 558: 531-539. https://doi.org/10.1038/s41586-018-0240-x

CONABIO. 2023. Portal de geoinformación. Comisión Nacional para el Conocimiento y Uso de la Biodiversidad, México. Available at: http://www.conabio.gob.mx/informacion/gis/ (accessed on March 20, 2023).

CONABIO. 2001. Climas de México de acuerdo a la clasificación de Koppen modificada por García (1998). Scale 1:1000000. Available at: http://www.conabio.gob.mx/informacion/gis/?vns=gis_root/clima/climas/clima1mgw (accessed on December 10, 2023).

Correa-Islas JJ, Romero-Padilla JM, Pérez-Rodríguez P, Vázquez-Alarcón A. 2023. Application of geostatistic models for aridity scenarios in northern Mexico. Atmósfera 37: 233-244. https://doi.org/10.20937/ATM.53103

Cui T, Zheng JZ, Zhang Z, Han Y, Huang D, Yang L, Chen S. 2025. Enhancing multi-model ensemble simulations of climate extremes over the Tibetan Plateau using machine learning. Theoretical and Applied Climatology 156: 390. https://doi.org/10.1007/s00704-025-05622-9

De Martonne E. 1926. Aréisme et indice d'aridité. Comptes Rendus de l'Académie des Sciences 182: 1395-1398.

Derdous O, Tachi SE, Bouguerra H. 2020. Spatial distribution and evaluation of aridity indices in Northern Algeria. Arid Land Research and Management 35: 1-14. https://doi.org/10.1080/15324982.2020.1796841

Descroix L, Loyer JY, Estrada-Ávalos J. 1993. Water resource in arid zones: The Hydrological Region 36 in northern México. In: IV International Conference on Desert Development: Sustainable Development for Our Common Future, Mexico City. Available at: https://www.researchgate.net/publication/32975378_Water_resource_in_arid_zones_the_hydrological_region_36_in_Northern_Mexico (accessed on December 6, 2024).

Eyring V, Bony S, Meehl GA, Senior CA, Stevens B, Stouffer RJ, Taylor KE. 2016. Overview of the Coupled Model Intercomparison Project Phase 6 (CMIP6) experimental design and organization. Geoscientific Model Development 9: 1937-1958. https://doi.org/10.5194/gmd-9-1937-2016

Ezquivel-Arriaga G, Nevarez-Favela MM, Velásquez-Valle MA, Sánchez-Cohen I, Bueno-Hurtado P. 2017. Hydrological modeling of a basin in Mexico's arid northern region and its response to environmental changes. Ingeniería Agrícola y Biosistemas 9: 3-17. http://doi.org/10.5154/r.inagbi.2016.12.008

FAO. 1996. Forest resources assessment 1990: Survey of tropical forest cover and study of change processes. FO: GCP/INT/550/USA. Food and Agriculture Organization of the United Nations. Available at https://www.fao.org/4/w0015e/W0015E00.htm#TOC (accessed on November 25, 2025).

Feng S, Fu Q. 2013. Expansion of global drylands under a warming climate. Atmospheric Chemistry and Physics Discussions 13: 10081-10094. https://doi.org/10.5194/acpd-13-14637-2013

Galloza MS, López-Santos A, Martínez-Santiago S. 2017. Predicting land at risk from wind erosion using an index-based framework under a climate change scenario in Durango, Mexico. Environmental Earth Sciences 76: 560. https://doi.org/10.1007/s12665-017-6751-1

García E. 2004. Modificaciones al sistema de clasificación climática de Köppen. Instituto de Geografía, Universidad Nacional Autónoma de México. Available at: https://publicaciones.geografia.unam.mx/index.php/ig/catalog/book/83 (accessed on February 5, 2025).

Gobie BG, Assamnew AD, Habtemicheal BA, Woldegiyorgis TA. 2024. Comparison of GCMs under CMIP5 and CMIP6 in reproducing observed precipitation in Ethiopia during rainy seasons. Earth Systems and Environment 8: 265-279. https://doi.org/10.1007/s41748-024-00394-0

González-Barrios JL, Vandervaere JP, Descroix L, Sánchez-Cohen I, Chávez-Ramírez E, González-Cervantes G. 2011. Impact of land use changes in surface hydrodynamics of a water-harvesting basin. In: Water resources in Mexico: Scarcity, degradation, stress, conflicts, management, and policy (Spring OU, Ed.). Hexagon Series on Human and Environmental Security and Peace 7: 167-176. https://doi.org/10.1007/978-3-642-05432-7_12

Graciano-Ávila G, Alanís-Rodríguez E, Aguirre-Calderón OA, González-Tagle MA, Treviño-Garza EJ, Mora-Olivo A, Buendía-Rodríguez E. 2019. Estimación de volumen, biomasa y contenido de carbono en un bosque de clima templado-frío de Durango, México. Revista Fitotecnia Mexicana 42: 119-127. https://doi.org/10.35196/rfm.2019.2.119

Haro A, Mendoza-Ponce A, Calderón-Bustamante Ó, Velasco JA, Estrada F. 2021. Evaluating Risk and possible adaptations to climate change under a socio-ecological system approach. Frontiers in Climate 3: 674693. https://doi.org/10.3389/fclim.2021.674693

Huang H, Winter JM, Osterberg EC, Horton RM, Beckage B. 2017. Total and extreme precipitation changes over the northeastern United States. Journal of Hydrometeorology 18: 1783-1798. https://doi.org/10.1175/JHM-D-16-0195.1

Huang J, Ji M, Xie Y, Wang S, He Y, Ran J. 2015a. Global semiarid climate change over last 60 years. Climate

Dynamics 46: 1131-1150. https://doi.org/10.1007/s00382-015-2636-8

Huang J, Yu H, Guan X, Wang G, Guo R. 2015b. Accelerated dryland expansion under climate change. Nature Climate Change 6: 166-171. https://doi.org/10.1038/nclimate2837

Huo Z, Dai X, Feng S, Kang S, Huang G. 2013. Effect of climate change on reference evapotranspiration and aridity index in arid region of China. Journal of Hydrology 492: 24-34. https://doi.org/10.1016/j.jhydrol.2013.04.011

IPCC. 1996. Revised 1996 IPCC guidelines for national greenhouse gas inventories. Reporting instructions (vol. 1). Intergovernmental Panel on Climate Change. Available at: https://www.ipcc-nggip.iges.or.jp/public/gl/invs4.html (accessed on March 30, 2024).

IPCC. 2014. 2013 revised supplementary methods and good practice guidance arising from the Kyoto Protocol (Hiraishi T, Krug T, Tanabe K, Srivastava N, Baasansuren J, Fukuda M, Troxler TG, Eds.). Intergovernmental Panel on Climate Change, Switzerland. Available at: https://www.ipcc.ch/site/assets/uploads/2018/03/KP_Supplement_Entire_Report.pdf (accessed on May 18, 2025).

Reddy S, Panichelli L, Waterworth RM, Federici S, Green C, Jonckheere I, Kahuri S, Kurz WA, de Ligt R, Ometto JP, Petersson H, Takahiro E, Paul T, Tullis J, Somogyi Z, Pandya M, Rocha MT, Suzuki K, eds. Chapter 3. Consisted representation of lands. In: 2019 refinement to the 2006 IPCC guidelines for national greenhouse gas inventories. Vol. 4: Agriculture, forestry and other land use (Calvo Buendia E, Tanabe K, Kranjc A, Baasansuren J, Fukuda M, Ngarize S, Osako A, Pyrozhenko Y, Shermanau P, Federici S, Eds.). Intergovernmental Panel on Climate Change, Switzerland. Available at: https://www.ipcc-nggip.iges.or.jp/public/2019rf/vol4.html (accessed on September 21, 2025).

IPCC. 2021. Summary for policymakers. In: Climate change 2021: The physical science basis. Contribution of Working Group I to the Sixth Assessment Report of the Intergovernmental Panel on Climate Change (Masson-Delmotte V, Zhai P, Pirani A, Connors SL, Péan C, Berger S, Caud N, Chen Y, Goldfarb L, Gomis MI, Huang M, Leitzell K, Lonnoy E, Matthews JBR, Maycock TK, Waterfield T, Yelekçi O, Yu R, Zhou B, Eds.). Cambridge University Press, Cambridge, United Kingdom and New York, 3-32. https://doi.org/10.1017/9781009157896.001

IPCC. 2022. Climate change: A threat to human wellbeing and health of the planet. Taking action now can secure our future. Intergovernmental Panel on Climate Change. Available at: http://www.ipcc.ch/2022/02/28/pr-wgii-ar6/ (accessed on December 20, 2024).

Jafarpour M, Adib A, Lotfirad M, Kisi Ö. 2023. Spatial evaluation of climate change-induced drought characteristics in different climates based on De Martonne Aridity Index in Iran. Applied Water Science 13: 133. https://doi.org/10.1007/s13201-023-01939-w

Jones GS, Andrews MB, Andrews T, Blockley E, Ciavarella A, Christidis N, Cotterill DF, Lott FC, Ridley J, Stott PA. 2024. The HadGEM3-GC3.1 contribution to the CMIP6 Detection and Attribution Model Intercomparison Project. Journal of Advances in Modeling Earth Systems 16: e2023MS004135. https://doi.org/10.1029/2023MS004135

Kalnay E, Cai M. 2003. Impact of urbanization and land-use change on climate. Nature 423: 528-531. https://doi.org/10.1038/nature01675

Lawrence TJ, Vilbig JM, Kangogo G, Fèvre EM, Deem SL, Gluecks I, Sagan V, Shacham E. 2023. Shifting climate zones and expanding tropical and arid climate regions across Kenya (1980-2020). Regional Environmental Change 23: 59. https://doi.org/10.1007/s10113-023-02055-w

Leija-Loredo EG, Valenzuela-Ceballos SI, Valencia-Castro M, Jiménez-González G, Castañeda-Gaytán G, Reyes-Hernández H, Mendoza-Cantú ME. 2020. Análisis de cambio en la cobertura vegetal y uso del suelo en la región centro-norte de México. El caso de la cuenca baja del río Nazas. Ecosistemas 29:1826. https://doi.org/10.7818/ECOS.1826

Li M, Wu P, Sexton DMH , Ma Z. 2021. Potential shifts in climate zones under a future global warming scenario using soil moisture classification. Climate Dynamics 56: 2071-2092. https://doi.org/10.1007/s00382-020-05576-w

López-Santos A, Pinto-Espinoza J, Ramírez-López EM, Martínez-Prado MA. 2013. Modeling the potential impact of climate change in northern Mexico using two environmental indicators. Atmósfera 26: 479-498.

López-Santos A, Martínez-Santiago S. 2015. Use of two indicators for the socio-environmental risk analysis of Northern Mexico under three climate change scenarios. Air Quality, Atmosphere and Health 8: 331-345. https://doi.org/10.1007/s11869-014-0286-3

Lugoi LP, Bamutaze Y, Martinsen V, Rossebø Almås A. 2023. Climate change hotpots and their implications

on rain-fed cropping systems in a tropical environment. Applied Geography 154: 102953. ISSN 0143-6228, https://doi.org/10.1016/j.apgeog.2023.102953

Martínez-Sifuentes AR, Turcíos-Caciano R, Rodríguez-Moreno VM, Villanueva-Díaz J, Estrada-Ávalos J. 2023. The impact of climate change on evapotranspiration and flow in a major basin in northern Mexico. Sustainability 15: 847. https://doi.org/10.3390/su15010847

Mojica-Guerrero AS, Trucíos-Caciano R, Valenzuela-Núñez LM, González-Barrios JL. 2009. Cambio en el uso de suelo en la cuenca del río Sextín. Tecnociencia Chihuahua 3: 121-130.

Monterroso-Rivas AI, Gómez-Díaz JD. 2021. Impacto del cambio climático en la evapotranspiración potencial y periodo de crecimiento en México. Terra Latinoamericana 39: e774. https://doi.org/10.28940/terra.v39i0.774

Morales-Estrada R. 2022. Análisis espaciotemporal del estudio de la dendrocronología en México. M.Sc. thesis. Universidad Autónoma Chapingo. Available at: https://repositorio.chapingo.edu.mx/server/api/core/bitstreams/7bff4b52-77a8-4726-8014-7a598e5d9a87/content (accessed on January 11, 2023).

Morales-Inocente MA, Nájera-Luna JA, Escobedo-Bretado A, Cruz-Cobos F, Hernández FJ, Vargas-Larreta B. 2020. Carbon retained in biomass and soil in forests at El Salto, Durango, Mexico. Investigación y Ciencia de la Universidad Autónoma de Aguascalientes 80: 5-13. https://doi.org/10.33064/iycuaa2020802997

Murray-Tortarolo GN, Jaramillo VJ, Larsen J. 2018. Food security and climate change: The case of rainfed maize production in Mexico. Agricultural and Forest Meteorology 253-254: 124-131. https://doi.org/10.1016/j.agrformet.2018.02.011

Neri C, Magaña V. 2016. Estimation of vulnerability and risk to meteorological drought in Mexico. Weather, Climate, and Society 8: 95-110. https://doi.org/10.1175/WCAS-D-15-0005.1

Oo HT, Zin WW, Thin Kyi CC. 2019. Assessment of future climate change projections using multiple global climate models. Civil Engineering Journal 5: 2152-2166. https://doi.org/10.28991/cej-2019-03091401

Ortega-Gaucin D, Bartolón J de la C, Castellano Bahena HV. 2018a. Drought vulnerability indices in Mexico. Water (Switzerland) 10: 1671. https://doi.org/10.3390/w10111671

Ortega-Gaucin D, Castellano HV, de la Cruz J. 2018b. Economic, social and environmental vulnerability to drought in the northwest river basin system, Mexico. International Journal of Environmental Impacts: Management, Mitigation and Recovery 1: 240-253. https://doi.org/10.2495/ei-v1-n3-240-253

Overpeck JT, Udall B. 2020. Climate change and the aridification of North America. Proceedings of the National Academy of Sciences 117: 11856-11858. https://doi.org/10.1073/pnas.2006323117

Pedroza-González E. 2011. Hidrometría ultrasónica en las presas "Lázaro Cárdenas" y "Francisco Zarco" en México. Ingeniería Hidráulica y Ambiental 32: 36-49.

Pellicone G, Caloiero T, Guagliardi I. 2019. The De Martonne aridity index in Calabria (southern Italy). Journal of Maps 15: 788-796. https://doi.org/10.1080/17445647.2019.1673840

Ríos-Romero A, Valdez-Cepeda RD, Torres-González JA, Navarrete-Molina C, López-Santos A. 2024. Climate change impact on rain-fed agriculture of northern Mexico. An analysis based on the CanESM5 model. Modeling Earth Systems and Environment 10: 3617-3631. https://doi.org/10.1007/s40808-024-01959-8

Salas-Quintanal H. 2011. El Río Nazas: la historia de un patrimonio lagunero. Instituto de Investigaciones Antropológicas, Universidad Nacional Autónoma de México, 70 pp. Available at: http://ru.iia.unam.mx:8080/handle/10684/19 (accessed on July 12, 2025).

Seager R, Ting M, Davis M, Cane M, Naik N, Nakumara J, Li C, Cook E, Stahle DW. 2009. Mexican drought: An observational modelling and tree ring study of variability and climate change. Atmósfera 22: 1-31.

SEMARNAT. 2008. Presas principales: uso y capacidad de almacenamiento. Secretaría del Medio Ambiente y Recursos Naturales, Mexico. Available at: https://apps1.semarnat.gob.mx:8443/dgeia/informe_2008/compendio_2008/compendio2008/10.100.8.236_8080/archivos/03_Dimension_ambiental/01_Agua/D3_AGUA01_07.pdf (accessed on October 1, 2023).

SEMARNAT. 2018. Acuerdo por el que se dan a conocer los valores de cada una de las variables que integran las fórmulas para determinar durante el ejercicio fiscal 2018 las zonas de disponibilidad, a que se refieren las fracciones I y II, del artículo 231 de la Ley Federal de Derechos, vigente a partir del 1 de enero de 2014. Secretaría de Medio Ambiente y Recursos Naturales, Mexico. Diario Oficial de la Federación, August 2.

SENARNAT. 2024. Decreto por el que se declara área natural protegida, con la categoría de área de protección de recursos naturales, el sitio Ríos y Montañas de la Comarca Lagunera, ubicada en los municipios

de Lerdo, Nazas, Mapimí, Cuencamé y Gómez Palacio, estado de Durango, y que abarca la superficie de 172,924-09-51.57 hectáreas. Secretaría de Medio Ambiente y Recursos Naturales, Mexico. Diario Oficial de la Federación, January 8.

Pinto Espinoza J, Martínez Prado MA, López Santos A, eds. 2012. Programa Estatal de Acción ante el Cambio Climático de Durango (PEACC-DURANGO). Secretaría de Recursos Naturales y Medio Ambiente del Estado de Durango, Victoria de Durango, 334 pp. Available at: https://medioambiente.durango.gob.mx/wp-content/uploads/sites/36/2022/02/peacc.pdf (accessed on October 12, 2024).

Rimal B, Zhang L, Keshtkar H, Haack BN, Rijal S, Zhang P. 2018. Land use/land cover dynamics and modeling of urban land expansion by the integration of cellular automata and Markov chain. ISPRS International Journal of Geo-Information 7: 154. https://doi.org/10.3390/ijgi7040154

Swart NC, Cole JNS, Kharin VV, Lazare M, Scinocca JF, Gillett NP, Anstey J, Arora V, Christian JR, Hanna S, Jiao Y, Lee WG, Majaess F, Saenko OA, Seiler C, Seinen C, Shao A, Sigmond M, Solheim L, von Salzen K, Yang D, Winter B. 2019. The Canadian Earth System Model v. 5 (CanESM5. 0.3). Geoscientific Model Development 12: 4823-4873. https://doi.org/10.5194/gmd-12-4823-2019

Tatebe H, Ogura T, Nitta T, Komuro Y, Ogochi K, Takemura T, Sudo K, Sekiguchi M, Abe M, Saito F, Chikira M, Watanabe S, Mori M, Hirota N, Kawatani Y, Mochizuki T, Yoshimura K, Takata K, O'ishi R, Yamazaki D, Suzuki T, Kurogi M, Kataoka T, Watanabe M , Kimoto M. 2019. Description and basic evaluation of simulated mean state, internal variability, and climate sensitivity in MIROC6. Geoscientific Model Development 12, 2727-2765. https://doi.org/10.5194/gmd-12-2727-2019

Troyo-Diéguez E, Mercado-Mancera G, Cruz-Falcón A, Nieto-Garibay A, Valdez-Cepeda RD, García-Hernández JL, Murillo-Amador B. 2014. Análisis de la sequía y desertificación mediante índices de aridez y estimación de la brecha hídrica en Baja California Sur, noroeste de México. Investigaciones Geográficas 85: 66-81. https://doi.org/10.14350/rig.32404

Ullah S, You Q, Sachindra DA, Nowosad M, Ullah W, Bhatti AS, Jin Z, Ali A. 2022. Spatiotemporal changes in global aridity in terms of multiple aridity indices: An assessment based on the CRU data. Atmospheric Research 268: 105998. https://doi.org/10.1016/j.atmosres.2021.105998

UNEP. 2019. Temperature rise is "locked-in" for the coming decades in the Arctic. United Nations Environment Programme. Available at: https://www.unep.org/news-and-stories/press-release/temperature-rise-locked-coming-decades-arctic#:~:text=-From%201979%20to%20the%20present%2C%20Arctic%20(,one%20third%20of%20sea%20level%20rise%20worldwide (accessed on July 1, 2025).

UNTFHS. 2017. Human security: Building resilience to climate threats. United Nations Trust Fund for Human Security, 4 pp. Avaliable at: http://www.un.org/humansecurity/wp-content/uploads/2017/10/Human-Security-and-Climate-Change-Policy-Brief-1.pdf (accessed on August 30, 2023).

Vlăduţ AŞ, Licurici M. 2020. Aridity conditions within the region of Oltenia (Romania) from 1961 to 2015. Theoretical and Applied Climatology 140: 589-602. https://doi.org/10.1007/s00704-020-03107-5

Voldoire A, Saint-Martin D, Sénési S, Decharme B, Alias A, Chevallier M, Colin J, Guérémy JF, Michou M, Moine MP, Nabat P, Roehrig R, Salas y Mélia D, Séferian R, Valcke S, Beau I, Belamari S, Berthet S, Cassou C, Cattiaux J, Deshayes J, Douville H, Ethé C, Franchistéguy L, Geoffroy O, Lévy C, Madec G, Meurdesoif Y, Msadek R, Ribes A, Sanchez-Gomez E, Terray L, Waldman R. 2019. Evaluation of CMIP6 DECK experiments with CNRM-CM6-1. Journal of Advances in Modeling Earth Systems 11: 2177-2213. https://doi.org/10.1029/2019MS001683

Wang J. 2020. Endorheic water. International encyclopedia of geography: People, the earth, environment and technology. https://doi.org/10.1002/9781118786352.wbieg2001

Williams KD, Copsey D, Blockley EW, Bodas-Salcedo A, Calvert D, Comer R, Davis P, Graham T, Hewitt HT, Hill R, Hyder P, Ineson S, Johns TC, Keen AB, Lee RW, Megann A, Milton SF, Rae JGL, Roberts MJ, Scaife AA, Schiemann R, Storkey D, Thorpe L, Watterson IG, Walters DN, West A, Wood RA, Woollings T, Xavier PK. 2018. The Met Office Global Coupled model 3.0 and 3.1 (GC3 and GC3.1) configurations. Journal of Advances in Modeling Earth Systems 10: 357-380. https://doi.org/10.1002/2017MS001115

WorldClim. Nd. Future climate data. Worldclim.org. Available at: https://www.worldclim.org/data/cmip6/cmip6climate.html (accessed on March 2023).

Xi H, Li T, Yuan Y, Chen Q, Wen Z. 2023. River ecosystem health assessment based on fuzzy logic and harmony degree evaluation in a human-dominated river basin. Ecosystem Health and Sustainability 9: 41. https://doi.org/10.34133/ehs.0041

Zhang X, Evans JP, Burrel AL. 2024. Less than 4% of dryland areas are projected to desertify despite increased aridity under climate change. Communications Earth & Environment 5: 300. https://doi.org/10.1038/s43247-024-01463-y

Supplementary material

Table SI. Integration of the Nazas River basin by municipalities from the Mexican states of Durango and Coahuila de Zaragoza.

State	Key	Name of the municipalities	Surface (km^2)	RI (%)
Durango	004	Cuencamé	3494	7.2
	007	Gómez Palacio	842	1.7
	008	Guadalupe Victoria	386	0.8
	010	Hidalgo	95	0.2
	012	Lerdo	1808	3.7
	013	Mapimí	5435	11.1
	015	Nazas	2387	4.9
	020	Pánuco de Coronado	368	0.8
	021	Peñón Blanco	1682	3.4
	024	Rodeo	1433	2.9
	028	San Juan del Río	1362	2.8
	029	San Luis del Cordero	605	1.2
	030	San Pedro del Gallo	1560	3.2
	036	Tlahualilo	3530	7.2
	001	Canatlán	976	2.0
	003	Coneto de Comonfort	1071	2.2
	005	Durango	806	1.7
	009	Guanaceví	3223	6.6
	011	Indé	2409	4.9
	017	Ocampo	272	0.6
	018	El Oro	3530	7.2
	025	San Bernardo	2276	4.7
	026	San Dimas	218	0.4
	035	Tepehuanes	3345	6.9
	032	Santiago Papasquiaro	3132	6.4
	039	Nuevo Ideal	258	0.5
Coahuila	009	Francisco I. Madero	689	1.4
	033	San Pedro	712	1.5
	017	Matamoros	545	1.1
	035	Torreón	302	0.6
	036	Viesca	37	0.1
		Total surface	48 788	

RI: relative importance.

Table SII. Details of the changes obtained according to the summed values of each of the intersection maps.

Details	Summed value	Details	Summed value
Remains as hyperarid	110	From subhumid changes to hyperarid	140
From hyperarid change to semiarid	210	From subhumid changes to semiarid	240
From hyperarid changes to Mediterranean semiarid	310	From subhumid changes to Mediterranean semiarid	340
From hyperarid changes to subhumid	410	Remains as subhumid	440
From hyperarid changes to humid	510	From subhumid changes to humid	540
From hyperarid changes to hyperumid	610	From subhumid changes to hyperumid	640
From semiarid changes to hyperarid	120	From humid changes to hyperarid	150
Remains as semiarid	220	From humid changes to semiarid	250
From semiarid changes to Mediterranean semiarid	320	From humid changes to Mediterranean semiarid	350
From semiarid changes to subhumid	420	From humid changes to subhumid	450
From semiarid changes to humid	520	Remains as humid	550
From semiarid changes to hyperumid	620	From humid changes to hyperumid	650
From Mediterranean semiarid changes to hyperarid	130	From hyperumid changes to hyperarid	160
From Mediterranean semiarid changes to semiarid	230	From hyperumid changes to semiarid	260
Remains as Mediterranean semiarid	330	From hyperumid changes to Mediterranean semiarid	360
From Mediterranean semiarid changes to subhumid	430	From hyperarid changes to Sub humid	460
From Mediterranean semiarid changes to humid	530	From hyperumid change to humid	560
From Mediterranean semiarid changes to hyperumid	630	Remains as hyperumid	660